

**On the Relationship Between ENSO and Extreme Weather  
Over the Contiguous United States**

Siegfried D. Schubert, Yehui Chang<sup>1</sup>, Max Suarez and Philip Pegion<sup>2</sup>  
NASA/GSFC, Earth-Sun Exploration Division  
Greenbelt, Maryland

30 August 2005

Submitted to US CLIVAR Variations

---

<sup>1</sup> Additional affiliation: Goddard Earth Sciences and Technology Center, University of Maryland Baltimore County, Baltimore, Maryland

<sup>2</sup> Additional affiliation: Science Applications International Corporation, Beltsville, Maryland

## 1. Introduction

Global-scale climate variations such as those associated with El Niño/Southern Oscillation (ENSO) are ultimately manifest in phenomena and processes that control regional-scale climates. For example, shifts in the wintertime planetary scale waves forced by tropical sea surface temperature (SST) anomalies can result in changes in the normal tracks and frequencies of storm systems (e.g. Noel and Changnon 1998) which can result in dramatic changes in regional climates of North America. Any potential changes in extreme weather events are of particular concern since these tend to have the greatest economic and social consequences. It is therefore of interest to determine whether the characteristics of extreme events are influenced by short-term climate variability such as that associated with ENSO. For example, Gershunov and Barnett (1998) and Gershunov (1998) show that the frequency of heavy rainfall is impacted by ENSO in a number of regions of the United States including the Great Plains, the Southeast, and the Gulf States. Cayan et al. (1999) show that ENSO impacts the occurrence of extreme (heavy) daily precipitation and stream flow throughout the western United States.

One limitation of many recent studies of weather extremes is that the analysis of the extreme events is carried out local in space, with little information provided about the underlying phenomenology and mechanisms associated with the extremes. In the case of precipitation, Web and Betancourt (1992) emphasize that understanding the hydroclimatic controls on flood frequency requires understanding the modulation of the flood generating mechanisms: for example, frontal systems, monsoonal flows and tropical storms. In that sense, identifying the impact on weather is an important step in determining the physical mechanisms by which short term climate variations impact extremes.

In this study, we examine the impact of ENSO on extreme precipitation events associated with winter storms over the continental United States. The results are based on observations (Higgins et al 1996), and an ensemble of nine atmospheric general circulation model (AGCM) simulations forced with observed SST for the 50-year period 1949-98. The AGCM is the NASA Seasonal to Interannual Prediction Project (NSIPP-1) model described in Bacmeister et al. (2000) and run

here at a resolution of 2° latitude by 2.5° longitude. The nine runs differ only in their initial atmospheric conditions: these were chosen arbitrarily from previously completed simulations.

An empirical orthogonal function (EOF) analysis of daily precipitation data is carried out separately for the observations and simulations to isolate the leading modes of precipitation variability. For both the observations and simulations, the first six rotated EOFs consist of localized precipitation anomalies that emphasize variability along the west coast, and the southern and southeast United States, and account for more than 50% of the variance over much of these regions. Various composite fields (e.g., 500mb heights) based on the time series of the corresponding principal components (PCs) show that the leading EOFs correspond to well-known storm systems. We focus here on those storms that contribute to extreme precipitation events along the gulf coast (the GC EOF) and the east coast (the EC EOF). These storms are well simulated, and the ensemble of runs provides a large sample of extreme events for statistical analysis. In the observations, the GC and EC storms show up as EOFs 3 and 4, respectively. In the EOF analysis of the model simulations, the GC and EC storms show up as EOFs 6 and 4, respectively. The model EOFs do have substantially less variance compared with the observed (the ratio of simulated to observed variance is 0.34 for the GC EOF and 0.45 for the EC EOF). This is likely a result of the relatively coarse resolution of the model.

## **2. The impact of ENSO**

In this section we examine the impact of ENSO on the extreme values of the PCs associated with the GC and EC EOFs. We begin by ordering the years according to the overall level of activity of the storms during each winter (measured by the variance of the PCs – see Table 1). Both the observations and simulations show a predilection for enhanced activity in the GC and EC storms during El Nino winters, while suppressed activity in the GC storm tends to occur during La Nina years. The simulated EC storms also tend to be suppressed during La Nina years, while that is less true for the observations.

Table 1: List of the winters (DJF) ordered by increasing variance for the GC and EC PCs from the observations and model simulations. Blue indicates La Nina years, and red indicates El Nino years. Bold indicates major events. Italics indicate weak events. The classification of the years into warm and cold events is that of the Climate Prediction Center (the classification scheme is subjective and is based on SST analyses; <http://www.nmic.noaa.gov>)

**GC(obs) GC(sim) EC (obs) EC(sim)**

<b>88-89</b>	<b>88-89</b>	<b>88-89</b>	<i>49-50</i>
<i>70-71</i>	<i>75-76</i>	<i>49-50</i>	59-60
93-94	<i>70-71</i>	<i>79-80</i>	<i>50-51</i>
<i>74-75</i>	<b>73-74</b>	85-86	<b>88-89</b>
<i>75-76</i>	<i>49-50</i>	<i>87-88</i>	<i>75-76</i>
59-60	59-60	<i>50-51</i>	<i>95-96</i>
61-62	53-54	56-57	<b>73-74</b>
<i>50-51</i>	60-61	<i>55-56</i>	60-61
<i>49-50</i>	<i>50-51</i>	<i>68-69</i>	52-53
67-68	96-97	80-81	<i>70-71</i>
62-63	<i>84-85</i>	51-52	<i>55-56</i>
56-57	<i>64-65</i>	<i>64-65</i>	80-81
85-86	<i>74-75</i>	<i>95-96</i>	85-86
<b>73-74</b>	<i>95-96</i>	61-62	71-72
<i>84-85</i>	<i>55-56</i>	<i>70-71</i>	89-90
<i>94-95</i>	78-79	<i>75-76</i>	<i>64-65</i>
<i>69-70</i>	80-81	52-53	51-52
<i>68-69</i>	<i>79-80</i>	62-63	61-62
<i>55-56</i>	56-57	76-77	78-79
<i>83-84</i>	71-72	96-97	<i>84-85</i>
52-53	66-67	53-54	<i>79-80</i>
89-90	62-63	93-94	<i>74-75</i>
<i>95-96</i>	<i>83-84</i>	60-61	81-82
60-61	67-68	67-68	<i>90-91</i>
96-97	63-64	71-72	53-54
66-67	85-86	<i>69-70</i>	96-97
<i>79-80</i>	<i>54-55</i>	<i>84-85</i>	62-63
<i>72-73</i>	89-90	<i>74-75</i>	56-57
71-72	81-82	<b>91-92</b>	66-67
80-81	<b>57-58</b>	<i>58-59</i>	63-64
51-52	51-52	<i>54-55</i>	<i>83-84</i>
<b>57-58</b>	<i>68-69</i>	<i>83-84</i>	<i>68-69</i>
81-82	<i>69-70</i>	89-90	<i>92-93</i>
63-64	<i>87-88</i>	<i>72-73</i>	<i>54-55</i>
<i>87-88</i>	52-53	<i>77-78</i>	67-68
53-54	<i>90-91</i>	<i>90-91</i>	<i>65-66</i>
<i>64-65</i>	<i>65-66</i>	66-67	<i>77-78</i>
<i>58-59</i>	<i>77-78</i>	<b>73-74</b>	<i>69-70</i>
76-77	61-62	<b>57-58</b>	<i>58-59</i>
<i>92-93</i>	<i>58-59</i>	<i>65-66</i>	<b>57-58</b>
<i>86-87</i>	76-77	81-82	<i>87-88</i>
<i>54-55</i>	93-94	<i>94-95</i>	76-77
<i>65-66</i>	<b>91-92</b>	<i>92-93</i>	<b>91-92</b>
<i>77-78</i>	<b>97-98</b>	63-64	<i>94-95</i>
78-79	<i>92-93</i>	<i>86-87</i>	<i>72-73</i>
<b>91-92</b>	<i>72-73</i>	59-60	<i>86-87</i>
<i>90-91</i>	<i>94-95</i>	78-79	93-94
<b>82-83</b>	<i>86-87</i>	<b>82-83</b>	<b>97-98</b>
<b>97-98</b>	<b>82-83</b>	<b>97-98</b>	<b>82-83</b>

We next examine how ENSO impacts the winter maxima by fitting the daily maxima to a class of extreme value distributions.. In particular, we fit the maximum values  $\{x\}$  to the Generalized Extreme Value (GEV) cumulative distribution function (Coles 2001)

$$G(x) = \exp\left\{-\left[1 + \xi\left(\frac{x - \mu}{\sigma}\right)\right]^{-1/\xi}\right\},$$

with location parameter ( $\mu$ ), scale parameter ( $\sigma$ ), and shape parameter  $\xi$ . Here  $\{x : 1 + \xi(x - \mu)/\sigma > 0\}$ ,  $-\infty < \mu, \xi < \infty$  and  $\sigma > 0$ . The Gumbel distribution ( $\xi = 0$ ) is one of three submodels of the GEV, the other two being the Frèchet ( $\xi > 0$ ) and reverse Weibull ( $\xi < 0$ ). The N-year return value for the GEV distribution (the value that is on average exceeded once in N-years) is,

$$X_N = \mu - \frac{\sigma}{\xi} \left\{1 - \left[-\ln\left(1 - \frac{1}{N}\right)\right]^{-\xi}\right\}.$$

We found that, for the observations, the Gumbel distribution provides a reasonable representation of the distribution of the maximum values of the PCs. On the other hand, we found that the reverse Weibull distribution provided the best fit to the leading *simulated* PCs. It is not clear whether this represents a real difference between the model and observations or whether the limited sample size (49 winters) of the observations is simply insufficient to produce a statistically significant estimate of the shape parameter.

In order to examine the impact of ENSO, we carry out the extreme value analysis separately for the La Nina, neutral and El Nino years. The impact of ENSO is quantified by computing an effective return period  $N^*$  (Katz et al. 2002), defined for the GEV distribution as

$$N^* \equiv \left\{1 - \exp\left(-\left[1 + \xi^* \frac{X_N - \mu^*}{\sigma^*}\right]^{-1/\xi^*}\right)\right\}^{-1},$$

where the star (\*) indicates conditional parameter values, and  $X_N$  is the unconditional N-year return value. For example, one might compute  $X_N$  from a full record, and then recalculate the parameters only for El Nino years. In that way one can more readily quantify the impact of El Nino in terms of the change in the return period.

The results for the GC and EC principal components are shown in Table 2. For the observations, only the location parameter,  $\mu$ , is impacted by ENSO – there are no significant impacts from ENSO on the scale parameter  $\sigma$ . In fact, we take advantage of this result by fixing the scale parameter to be that estimated from the full (unconditional) record, thereby reducing the number of free parameters in the final fit. Both the GC and EC storms have significantly different location parameters during cold and warm years. The impact is quantified in the last column in Table 3 in terms of the impact on the return values. The results are such that observed extreme GC and EC storms that occur on average only once every 20 years (20-year storms) would occur on average in half that time under El Nino conditions. In contrast, under La Nina conditions, 20-year GC and EC storms would occur on average about once in 30 years. The results are quite similar for the *simulated* GC storms in that the 20-year return values would occur on average in half that time during warm years, and twice that time during cold years. For the EC storms the 20-year return value would also occur in half that time under warm conditions and in about twice that time under cold conditions.

Figure 1 shows the results of fitting Gumbel distributions to the observations and each of the 9 ensemble members. We choose here to fit the simpler Gumbel distribution to the model results since, by doing the fits to the individual ensemble members, we are limiting the sample size to that of the observations. The scatter among the ensemble members gives an indication of the sampling errors. The fact that the fit to the observations falls within the scatter suggests that the model results are quite realistic. The results also show that the impact from ENSO clearly separates the warm and cold years (despite the sampling errors), with La Nina years tending to produce considerably less intense extremes than the El Nino years.

Fig. 2 is the same as Fig. 1, except for the EC storms. Here again we see that the fits to the observed values fall within the scatter of the fits to the individual ensemble members. The cold and warm years are also clearly separated, though in this case there is considerably more scatter in the results for the warm years, with some ensemble members showing a quite broad distribution, while others are more narrow and peaked.

**Table 2:** The parameter estimates of the GEV distribution for the EC and GC PCs from the observations and model simulations. Values are based on the maximum daily values during DJF based on either the 50 (1949-98) observed winters or the 450 simulated winters comprised of nine ensemble members times fifty (1949-98) years. Separate fits are done for La Nina, neutral and El Nino winters. For the observations, the values in parentheses are the 90% confidence intervals based on 2000 Monte Carlo simulations. For the simulations, the values in parentheses are the standard errors. Parameter values ( $\mu$ ,  $\sigma$ ) are normalized by the standard deviation of the PCs. The last column shows the effective return period (in years) that the  $X_{20}$  value would have under warm, cold, or neutral ENSO conditions. The results were computed using either the *XTREMES* software package (Reiss and Thomas 1997), or the *extRemes* software described at <http://www.assessment.ucar.edu/toolkit/index.html>.

PC	ENSO	$\mu$ -location	$\sigma$ -scale	$\xi$ -shape	N*
	cold	3.71 (3.1, 4.6)	1.59		30.0
GC (obs)	neutral	4.30 (3.8, 4.9)	1.59		20.9
	warm	5.26 (4.7, 6.1)	1.59		11.6
	cold	3.37 (0.16)	1.57 (0.12)	-0.04 (0.08)	33
GC(sim)	neutral	4.29 (0.14)	1.76 (0.10)	-0.16 (0.05)	28
	warm	5.18 (0.18)	1.88 (0.12)	-0.15 (0.06)	10
	cold	3.49 (3.0, 4.2)	1.25		29.7
EC(obs)	neutral	4.09 (3.7, 4.6)	1.25		18.7
	warm	4.77 (4.3, 5.3)	1.25		11.0
	cold	3.81 (0.13)	1.34 (0.09)	-0.06 (0.05)	43
EC(sim)	neutral	4.13 (0.11)	1.38 (0.08)	-0.04 (0.04)	26
	warm	5.05 (0.15)	1.58 (0.09)	-0.10 (0.03)	11

*Acknowledgements:* This work was supported by the NASA Earth Science Enterprise's Global Modeling and Analysis Program.

## References

- Bacmeister, J., P.J. Pegion, S. D. Schubert, and M.J. Suarez, 2000: An atlas of seasonal means simulated by the NSIPP 1 atmospheric GCM, NASA Tech. Memo. No. 104606, volume 17, Goddard Space Flight Center, Greenbelt, MD 20771, 2000.
- Cayan, D. R., K.T. Redmond, and L.G. Riddle, 1999: ENSO and hydrological extremes in the western United States. *J. Climate*, 12, 2881-2893.
- Coles, S. 2001: *An Introduction to Statistical Modeling of Extreme Values*. Springer Verlag, London.
- Gershunov, A., 1998: ENSO influence on intraseasonal extreme rainfall and temperature frequencies in the contiguous United States: Implications for long-range predictability. *J. Climate*, 11, 3192-3203.
- Gershunov, A. and T.P. Barnett, 1998: ENSO influence on intraseasonal extreme rainfall and temperature frequencies in the contiguous United States: Observations and model results. *J. Climate*, 11, 1575-1586.
- Higgins, R. W., J. E. Janowiak and Y. Yao, 1996: A gridded hourly precipitation data base for the United States (1963-93). *NCEP/Climate Prediction Center, Atlas No. 1*.
- Kalnay, E., and Coauthors, 1996: The NCEP/NCAR 40-year reanalysis project. *Bull. Amer.Meteor.Soc.*, 77, 437-471.
- Katz, Richard W., Parlange, Marc B. and Naveau, Philippe, 2002: Statistics of extremes in hydrology. *Advances in Water Resources*, 25, 1287–1304.
- Noel, J. and D. Changnon, 1998: A pilot study examining U.S. winter cyclone frequency patterns associated with three ENSO parameters. *J. Climate*, 11, 2152-2159.

Reiss, R.-D., and M. Thomas, 1997: Statistical Analysis of Extreme Values. Birkhäuser, Basel, 316 pp.

Webb, R.H. and J.L. Betancourt, 1992: Climate variability and flood frequency of the Santa Cruz River, Pima County, Arizona. U.S. Geological Survey, Water-Supply Paper, 2379. 40pp.

Yarnal, B. and H.F. Diaz, 1986: Relationships between extremes of the Southern Oscillation and the winter climate of the Anglo-American Pacific coast. *J. Climatol.*, 6, 197-219.

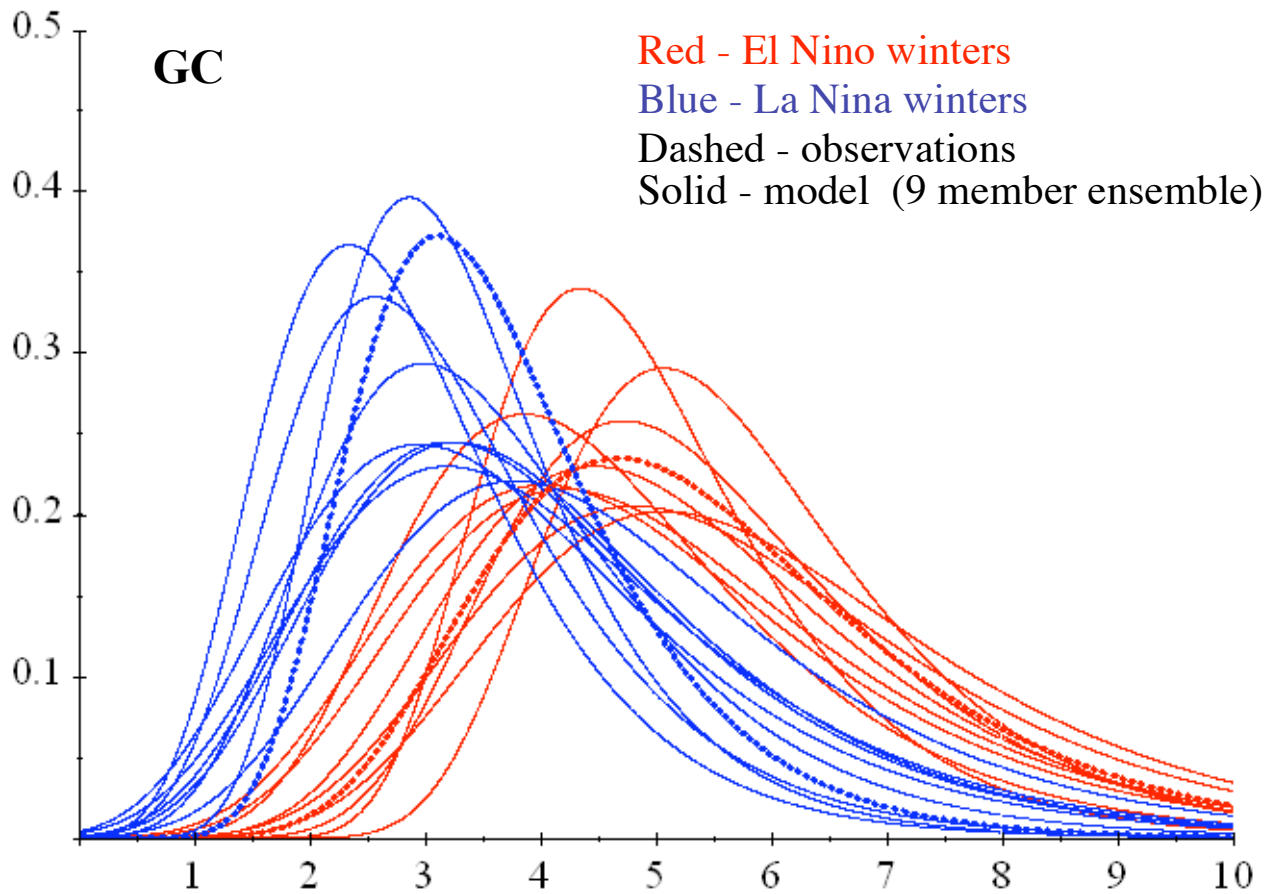


Figure 1: Probability Density Functions (PDFs) of extreme winter storms that tend to develop along the Gulf Coast (GC) during DJF (1949-1998). The PDFs correspond to the maximum value of the principal components associated with EOF 3 (observations) and EOF 6 (model). Values are scaled so that the model and observed EOFs have the same total variance. Units are arbitrary. The PDFs are the fits to a Gumbel Distribution. The analysis was done using the *XTREMES* software package (Reiss and Thomas 1997).

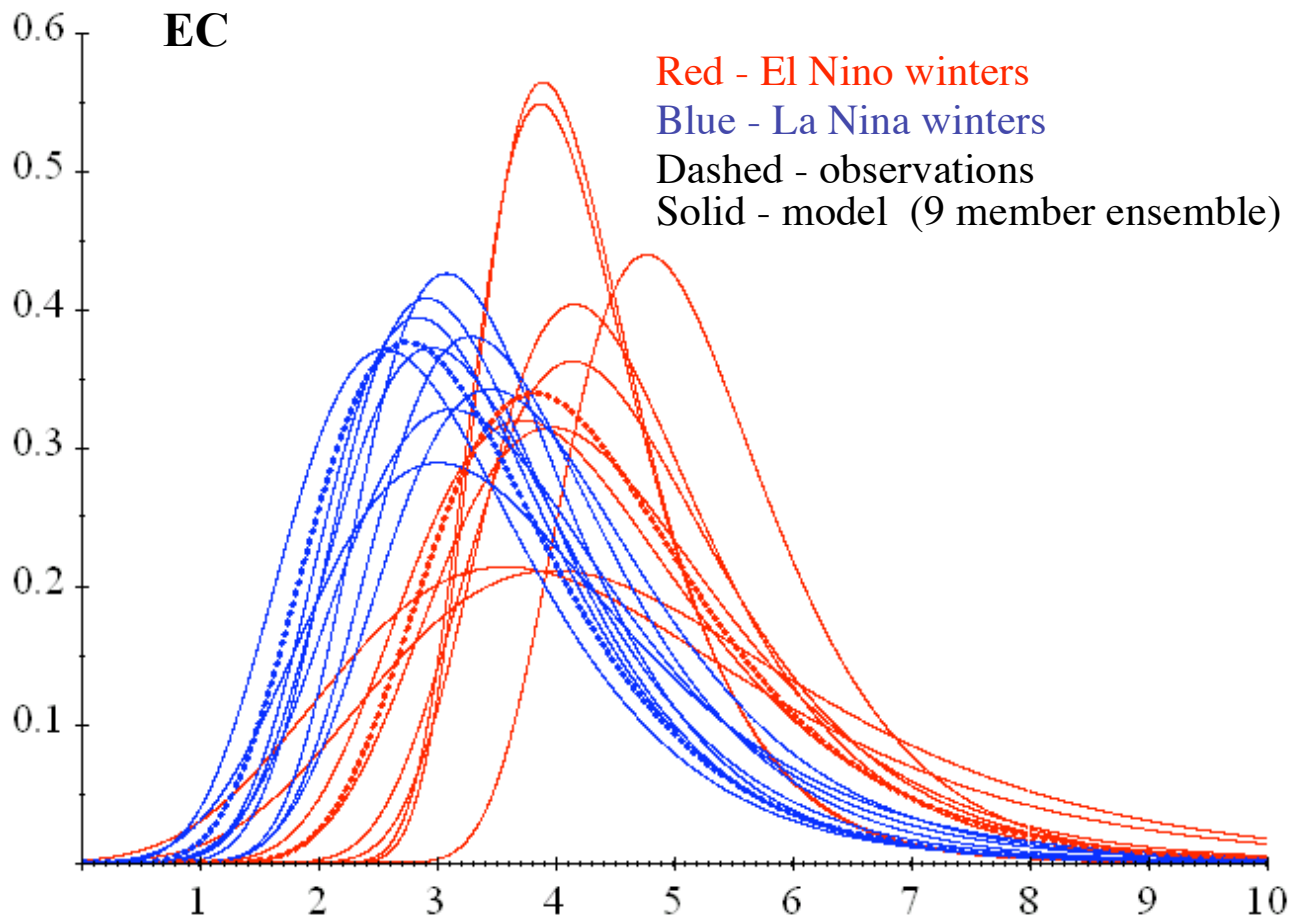


Figure 2: Same as Fig.1, except for the extreme winter storms that develop along the east coast (EC). The PDFs correspond to the maximum value of the principal components associated with EOF 4 (observations) and EOF 4 (model).